Auroral Signatures of Ionosphere-Magnetosphere Coupling at Jupiter and Saturn

L. C. Ray

Space and Atmospheres Group, Department of Physics, Imperial College London, London, UK

R. E. Ergun

Laboratory for Atmospheric and Space Physics, University of Colorado, Boulder, Colorado, USA

Department of Astrophysical and Planetary Sciences, University of Colorado, Boulder, Colorado, USA

Planetary auroral emissions are an observable signature of the coupling between the planetary magnetosphere and ionosphere. Jovian and Saturnian auroral emissions are created by a variety of processes, including those driven by the orbital motions of moons through the planetary magnetic plasma, the local creation, and subsequent pickup of plasma in the inner magnetosphere, due to the geologically active moons Io and Enceladus, respectively, and the radial transport of plasma through the middle and outer magnetosphere. Along with these internally driven phenomena, there exist auroral emissions owing to the global interaction of the planetary magnetosphere such as the release of plasma down the magnetotail. The current understanding of Jovian and Saturnian auroral processes is derived from attempting to reconcile theoretical models of ionosphere-magnetosphere coupling with physical parameters derived from auroral observations and in situ magnetospheric data. We focus on the processes limiting the strength of the ionosphere-magnetosphere coupling that predominantly occur in the ionosphere and at high latitudes along the magnetic field line.

1. INTRODUCTION

1.1. Internally Driven Magnetospheres

The Jovian and Saturnian magnetospheres have significant internal plasma sources due to their respective moons Io and Enceladus. Io orbits Jupiter at a distance of 5.9 R_J (Jovian radii) and is the most volcanically active body in the solar system outgassing ~700–3000 kg s^{-1} of neutral material, predominately sulfur dioxide, into the Jovian magnetosphere. Roughly half of this mass leaves the magnetosphere through charge exchange and fast neutral escape [*Delamere et al.*, 2005]. The remaining ~350–1500 kg s^{-1} of plasma, composed of ionized oxygen, sulfur, and mixed compounds, populates the dense Io torus and, after a torus-residence lifetime of ~14–60 days, is transported radially outward through the magnetosphere, eventually being lost down the magnetotail of the planet (see reviews by *Thomas et al.* [2004] and *Bagenal and Delamere* [2011]). The radial profile of the plasma angular velocity stays near the planetary rotation rate (Ω_{Jup} = 1.76 × 10^{-4} rad s^{-1}) out to ~17–20 R_J beyond which it departs significantly from this value [*McNutt et al.*, 1979]. Outside of ~15 R_J, the planetary magnetic field is distended by the current sheet created by the ion and azimuthal drift motions of the plasma. Additionally, the high-beta plasma population, $\beta > 10$ outside ~22 R_J [*Mauk et al.*, 2004], inflates the Jovian magnetosphere, expanding the system to observable subsolar magnetopause

Auroral Phenomenology and Magnetospheric Processes: Earth and Other Planets
Geophysical Monograph Series 197

10.1029/2011GM001172

distances from the planetary center of 63 R_J (during high-pressure solar wind) or 92 R_J (during low-pressure solar wind) rather than the ~43 R_J that one would predict from simple pressure balance between the planetary magnetic field and the solar wind ram pressure [*Joy et al.*, 2002].

The Saturnian moon Enceladus has a more moderate neutral outgassing rate of ~150–300 kg s^{-1} [*Hansen et al.*, 2006], primarily composed of water group molecules. The dominant ionization process is charge exchange, narrowly surpassing the combination of photoionization and electron impact ionization [*Fleshman et al.*, 2010]. Estimates of the plasma radial mass transport rate range from ~10s of kg s^{-1} to 280 kg s^{-1} (see review by *Bagenal and Delamere* [2011]). Interestingly, the radial profile of the magnetospheric plasma angular velocity shows a 20% departure from corotation outside ~4 R_S (Saturnian radii) [*Wilson et al.*, 2009]. Outside ~6 R_S, Saturn's magnetic field is radially "stretched" owing to magnetic contribution of the ring current. Past 9 R_S, the Saturnian magnetosphere becomes inflated due to internal high-beta plasma pressure, $\beta > 1$ [*Sergis et al.*, 2010], but to a lesser extent than the Jovian system. At Saturn, the observed subsolar magnetopause distances are typically 22 or 27 R_S for high- or low-pressure solar wind conditions, respectively, instead of the ~19 R_S predicted by a vacuum dipole magnetic field.

1.2. Auroral Emissions

There are three types of auroral emission observed on Jupiter, each driven by a different process (see review by *Clarke* [this volume]). These are (1) satellite aurorae, which are exemplified by the Io footprint and wake emission, Ganymede and Europa footprints, (2) the constant main aurora ("main oval"), which consists of a "ring" of emission, and (3) the variable polar emissions, which are observed poleward of the main emission. Both the internally driven satellite wake emission and the main auroral emission are signatures of steady state ionosphere-magnetosphere coupling and are the focus of this chapter.

Jupiter's satellite aurorae are created by the motion of satellites through the rapidly rotating magnetospheric plasma. The auroral emission associated with Io is the brightest and most interesting of the three satellite signatures (Io, Ganymede, and Europa). Io's auroral emission can be split into two distinct regions: the instantaneous Io spot and the steady state wake emission. The Io spot is created by an Alfvénic disturbance imposed by the Io obstacle upon the magnetic flux tube sweeping past the moon (see reviews by *Saur* [2004], *Bonfond* [this volume], and *Hess and Delamere* [this volume]). In the frame corotating with Jupiter, Io orbits with a velocity of -57 km s^{-1}, and hence, the Io-driven auroral emissions have a retrograde relative motion. The Io wake emission is caused by the steady state current system, which is set up to transfer angular momentum from Jupiter to the local wake plasma. These currents impose a force that accelerates the plasma, which has been diverted around the obstacle, back up to corotation [*Hill and Vasyliūnas*, 2002; *Ergun et al.*, 2009]. The wake emission persists far downstream of the Io spot. Observations of the Io spot show that the mean energy of the associated precipitating electrons is ~55 keV [*Gérard et al.*, 2002]. Recent observations of the Io wake find a lower mean electron energy of ~1 keV [*Bonfond et al.*, 2009] (see Table 1).

The main auroral emission is the signature of the steady state, global current system transferring angular momentum from Jupiter to outward moving plasma. Observations of the main auroral emission show a persistent structure, which is fixed to Jupiter's longitudinal coordinate system, System III, and maps to an equatorial distance of 20–30 R_J [e.g., *Khurana*, 2001; *Clarke et al.*, 2004]. There are some variations in the main auroral emission, but it is difficult to determine whether these are due to local time effects or variations in the magnetic field structure with System III longitude as the aurora is preferentially observed on the dayside between 155° and 270° central meridian longitude (CML) [*Grodent et al.*, 2003a]. *Grodent et al.* [2003a] determined that the Jovian magnetic field controls some aspects of the main auroral emission, with the location of the auroral emission contracting toward the poles as the CML increases from 115° to 255°. *Gustin et al.* [2004] found a mean precipitating electron energy of ~30–200 keV and incident energy flux of ~2–30 mW m^{-2} for the main auroral emission. However, there are some aspects of the main auroral emission that are more clearly fixed in local time. *Radioti et al.* [2008] showed that the main auroral emission has a persistent dark region in the prenoon to noon sector, thought to be the signature of a downward current, perhaps representing closure or return currents not associated with downward precipitating electrons. Additionally, there are often bright morning storms observed in the dawn sector. The bright morning aurora is caused by much more energetic electrons with precipitating energies as large as ~460 keV and associated incident energy fluxes in the order of 100 mW m^{-2} [*Gustin et al.*, 2006]. In addition to magnetic and local time variations, the main auroral emission has been observed to shift up to 3° in latitude over time [*Grodent et al.*, 2008] and to vary with solar wind conditions [*Nichols et al.*, 2007; *Cowley et al.*, 2007; *Yates et al.*, 2012; *Delamere*, this volume].

Saturn's internally driven auroral emissions are not yet definitively identified with their corresponding magnetospheric driver and, in comparison to the Jovian system, possibly sedate. Enceladus' auroral footprint was recently

Table 1. Auroral Features With Associated Precipitating Electron Properties

Auroral Feature	Associated Process and Location[a]	Precipitating Energy Flux (mW m^{-2})	Mean Electron Energy (keV)
	Jupiter		
Io footprint	Alfvénic; $6R_J$	33[b]	55[b]
Io wake	Acceleration of wake plasma; $6R_J$	2–20[c]	1–2[c]
Main oval	Radial transport of iogenic plasma	2–30[d]	30–200[d]
Polar aurora	?	0–200[e]	?
	Saturn		
Enceladus footprint	Alfvénic; $4R_S$	0.15–0.45[f]	?
Diffuse emission	$4–11R_S$	~0.3[g]	~1[g]
Main emission	Interaction with SW; $\sim 20R_S$	0.2–1.4[h]	10–18[i]

[a]Location of auroral process when mapped to the magnetosphere.
[b]*Gerard et al.* [2002].
[c]*Bonfond et al.* [2009].
[d]*Gustin et al.* [2004].
[e]Polar emission is highly variable. See discussion of *Grodent et al.* [2003b].
[f]Derived from the work of *Pryor et al.* [2011] using 1 kR = 10 mW m^{-2}.
[g]*Grodent et al.* [2010].
[h]Derived from the work of *Gustin et al.* [2009] using 1 kR = 10 mW m^{-2}.
[i]*Gustin et al.* [2009].

discovered after years of dedicated observations and is only present in a few percent of available images [*Pryor et al.*, 2011]. While there is indication of a satellite footprint, there have not yet been observations of an associated wake emission, as with the Io interaction at Jupiter. Poleward of the Enceladus footprint is a region of diffuse auroral emission, which maps to ~4–11 R_S in the magnetosphere and is consistent with electron precipitation from pitch-angle scattering of the suprathermal magnetospheric electron population [*Grodent et al.*, 2010]. However, while not yet extensively studied, this emission could also be a signature of momentum loading in the Saturnian magnetosphere. The magnetospheric plasma's angular velocity profile lags corotation outside ~3.3 R_S [*Wilson et al.*, 2009] owing to both the charge exchange between ion and neutrals and radial transport of plasma [*Saur et al.*, 2004; *Pontius and Hill*, 2009]. The brightest UV auroral signature maps to the outer magnetosphere, varying with solar wind conditions. Yet it is not clear whether the emission is the signature of field-aligned currents enforcing corotation [*Sittler et al.*, 2006] or those caused by the rotational shear flow at the open-closed boundary of the magnetopause [*Cowley et al.*, 2008; *Bunce*, this volume].

So the question is, Why does the Jovian magnetosphere have such strong auroral signatures of ionosphere-magnetosphere coupling that are clearly internally driven, while uncertainty still remains regarding the drivers for Saturn's auroral emissions? Within both magnetospheres, there exists an active moon, which populates the system with neutral particles that are subsequently ionized, picked up by the planetary magnetic field, and transported radially outward. Both magnetospheres are inflated by their internal plasma population beyond what would be predicted by simple pressure balance between the planetary magnetic field and the solar wind ram pressure, as detailed in Table 2, and both magnetospheres are rapid rotators. However, the Saturnian magnetic field is ~20 times weaker than Jupiter's, and the upper atmosphere is more extended, due to Saturn having one third the Jovian mass and, hence, a correspondingly smaller gravitational field.

Table 2. Basic Parameters of Earth and Jupiter and Saturn

	Earth	Jupiter	Saturn
Orbital distance (AU)	1	5.2	9.5
Planetary mass (10^{24} kg)	5.9736	1,898.6	568.46
Equatorial radius (km)	6,378	71,400	60,268
Equatorial field strength (gauss)	0.3	4.2	0.2
Dipole direction (geographic)	S to N	N to S	N to S
Magnetic tilt (°)	11	9.4	<1
Rotational period (h)	24	9.9	10.7
Magnetopause distance estimated from magnetic field and solar wind pressure balance (R_P)	10.2	42.6	18.9
Observed magnetopause distance (R_P)	10	63;92[a]	22;27[b]
Auroral ionospheric Pedersen conductance (mho)	2–3	~0.1–1s	1–10s

[a]Magnetopause standoff distance has a bimodal distribution corresponding to compressed and relaxed states [*Joy et al.*, 2002].
[b]*Achilleos et al.* [2008].

2. ANGULAR MOMENTUM TRANSFER

The auroral emissions detailed above are signatures of the transfer of angular momentum from the parent planet to its surrounding magnetospheric plasma. The current system that facilitates this transfer is briefly described below, and the reader is referred to more detailed works for completeness [e.g., *Hill*, 1979; *Pontius and Hill*, 1982; *Hill*, 2001; *Hill and Vasyliūnas*, 2002; *Cowley and Bunce*, 2001, 2003; *Nichols and Cowley*, 2004; *Ergun et al.*, 2009; *Ray et al.*, 2010; *Nichols*, 2011]. In the first case of the Io wake emission, the plasma population requiring angular momentum is newly created plasma that, as a previously neutral molecule or atom, orbited Jupiter at the local Keplerian velocity. Upon ionization, the plasma is picked up by the planetary magnetic field, which is tied to the planet's rotation rate. As the background plasma has a nonzero velocity relative to the magnetic field, there exists a motional electric field ($\mathbf{E} = -\mathbf{v} \times \mathbf{B}$) in the radial direction, which maps to a latitudinal electric field in the planetary ionosphere. The ionospheric electric field corresponds to an associated latitudinal current, which diverges to flow out from the planet along the magnetic field and then radially outward in the equatorial plane, eventually returning to the planet along the magnetic field to close the circuit. The upward field-aligned currents communicate angular momentum from Jupiter to the magnetospheric plasma, with the radial current providing a $\mathbf{J} \times \mathbf{B}$ force in the rotational direction that accelerates the plasma from its initial Keplerian velocity to a combined gyration/drift motion where the guiding center angular velocity approaches corotation with the planet. Current-carrying electrons precipitate into Jupiter's atmosphere, resulting in the Io wake emission. As the plasma nears corotation, the field-aligned currents transferring angular momentum subside, and the auroral emission decays. Figure 1 displays the full current circuit. The magnitude of the angular momentum transfer in the Io wake region is primarily dictated by the Pedersen conductance at the foot of the planetary magnetic field in the Jovian ionosphere. Observations show that the Io wake can extend as much as 120° in longitude downstream from the Io footprint.

This process most assuredly happens in the Saturnian system when water group molecules from Enceladus are ionized, yet there is no corresponding, detectable wake auroral signature suggesting that at Enceladus' orbit, the pickup currents are weaker than in the Jovian case. However, the ionization of neutral particles from Enceladus spans a broad radial range in the magnetosphere from ~4 to 8 R_S. Therefore, it is possible that the inner portion of the diffuse auroral emission is related to the pickup of these newly created ions.

In the next cases of the Jovian main auroral emission, and possibly both the outer region of the Saturnian diffuse aurora and the main auroral emission, these are signatures of plasma from Io or Enceladus, respectively, being transported radially outward through the parent magnetosphere. As the plasma moves outward, conservation of angular momentum dictates that it slows down. However, in the collisionless MHD approximation, the plasma is frozen into the magnetic field, and the deviation from the planetary rotation rate results in the field lines being azimuthally "bent back" near the equator.

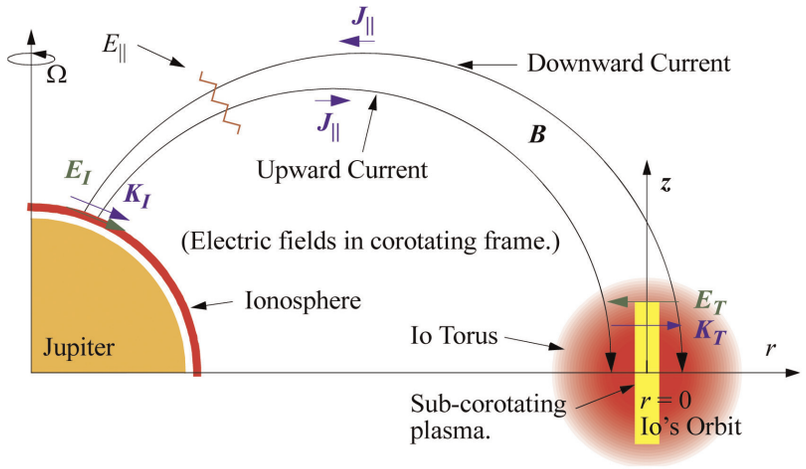

Figure 1. Current system associated with angular momentum transport in the Io wake region. $K_{I/T}$ is the height-integrated current density in the ionosphere/magnetosphere, $E_{I/T}$ is the perpendicular electric field in the ionosphere/magnetosphere, $J_\parallel$ is the field-aligned current, and $E_\parallel$ is the parallel electric field that develops at high latitudes. From the work of *Ergun et al.* [2009].

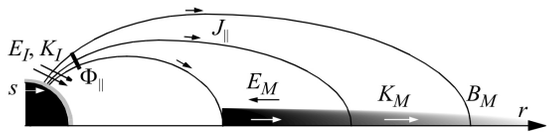

Figure 2. Upward current system associated with angular momentum transport due to radially moving plasma. $K_{I/M}$ is the height-integrated current density in the ionosphere/magnetosphere, $E_{I/M}$ is the perpendicular electric field in the ionosphere/magnetosphere, $J_\parallel$ is the field-aligned current, and $\Phi_\parallel$ is the parallel electric field that develops at high latitudes. From the work of *Ray et al.* [2010].

The curl of this field configuration is a radially outward current in the equatorial magnetosphere, closed by field-aligned currents that run between the ionosphere and magnetosphere, transferring angular momentum as shown in Figure 2. The motional electric field of the rotating magnetospheric plasma is, in a sense, "mapped" along magnetospheric field lines between these regions and, thus, partially drives ionospheric current. In the magnetosphere, the equatorial $\mathbf{J} \times \mathbf{B}$ force accelerates the plasma toward corotation, which diminishes the magnetospheric electric field. Yet unlike the case of local plasma pickup where the current system evolves in azimuth at a constant magnetospheric radius and therefore maps to a region of fairly constant magnetic field strength, here the magnetic field strength decreases as the current system evolves with radial distance from the planet. This means that at a certain radial distance, the planet will no longer be able to supply the necessary angular momentum to keep the magnetospheric plasma near corotation. When this happens, significant subcorotation of the plasma ensues. Again, the corresponding auroral emission is created by the excitation of atmospheric molecules by precipitating electrons that carry the field-aligned current between the planet and magnetospheric plasma.

There are two factors, however, which limit the current systems described above: finite ionospheric Pedersen conductance and the lack of current carriers at high latitudes along the magnetic field line. It is the interplay between these two factors that quantitatively dictates the location and intensity of the auroral emission.

2.1. Ionospheric Pedersen Conductance

The ionospheric Pedersen conductance, Σ_P, also known as the height-integrated Pedersen conductivity, controls the current density that flows through the ionosphere for the above current systems. The Pedersen conductance is associated with particle mobility in the direction parallel to the ionospheric electric field and perpendicular to the planetary magnetic field. The local Pedersen conductivity maximizes at the altitude where the ion gyrofrequency equals the ion-neutral collision frequency. Assuming that the ionospheric electric field can be described by a simplified Ohm's law as $\mathbf{E_I} = \mathbf{K_I}/\Sigma_P$, where $\mathbf{K_I}$ is the height-integrated ionospheric current density, a small Σ_P for a fixed ionospheric electric field will decrease the magnitude of the currents that can flow through the ionosphere. This also implies that small Pedersen conductances result in relatively weak closure currents flowing between the ionosphere and magnetosphere transferring angular momentum. For low Σ_P, the magnetospheric plasma will not receive the angular momentum necessary to return toward corotation and will persistently lag the planetary rotation rate. On the other hand, for a large Σ_P, the ionosphere will readily provide the currents necessary to accelerate the magnetospheric plasma toward corotation, and we would expect the plasma to rotate closer to the planetary rate over a more extended range in radial distance.

Ideally, the ionosphere and upper neutral atmosphere would have the same rotation frequency as Jupiter's deep interior. However, at high altitudes, the ionosphere slips in its rotation due to the torque exerted on it by the currents feeding angular momentum from the ionosphere to the magnetosphere. This, in turn, reduces the rotation rate of the neutral atmosphere through ion-neutral collisions. At low altitudes, the slowing of the neutral atmosphere through ion-neutral collisions is less efficient as angular momentum is more readily transported from the deep planetary interior to the neutral atmosphere. The net result is that the low altitude ionosphere rotates near or at the planetary rotation rate, while the rotation rate of the upper ionosphere more closely reflects that of the magnetospheric plasma [*Huang and Hill*, 1989]. It is, therefore, common to discuss an "effective" conductance, which is the true Pedersen conductance reduced to account for the subcorotation of the neutral atmosphere and, hence, ionosphere in the upper atmosphere.

The ionospheric Pedersen conductances in Saturn's auroral regions are determined by combining radio occultation data with models of the neutral atmosphere and ionosphere. Calculations of the "true" Pedersen conductance range from ~1 to 10s of mho [*Moore et al.*, 2010; *Galand et al.*, 2011]. On Jupiter, estimates of the "true" Pedersen conductance range from ~0.1 to ~8 mho [*Millward et al.*, 2002] and are predominately based on modeling efforts of the atmosphere and ionosphere-magnetosphere system.

2.2. High-Latitude Plasma Density

The second restriction on the ionosphere-magnetosphere coupling current system is the centrifugal confinement of the magnetospheric plasma due to the rapid plasma rotation rate. On Jupiter, heavy ions are confined near the centrifugal

equator due to large centrifugal forces [*Hill and Michel*, 1976]. While the electrons are less confined due to their smaller mass, their mobility along the magnetic field line is restricted by an ambipolar electric field, which is set up to maintain quasi-neutrality of the plasma. As the ionospheric plasma is confined to the planet due to strong gravitational forces, this restriction in the magnetospheric electron mobility leads to a lack of current-carrying plasma at high latitudes as shown in Figure 3. Consequently, field-aligned potentials develop at high magnetic latitudes to augment the electron distribution in the loss cone and, thus, increase the field-aligned current that can flow between the ionosphere and magnetosphere. The resulting current-voltage relation that describes the change in field-aligned current with field-aligned potential is nonlinear and depends on the density and temperature of the electron population at high latitudes as well as the mirror ratio at the top of the acceleration region [*Knight*, 1973; *Ray et al.*, 2009]. For the Io flux tube, the acceleration region forms at ~2.5 R_J jovicentric distance. Theoretically, it is possible for the field-aligned current density to saturate; that is, the entire electron distribution is accelerated into the loss cone such that the current density is maximized, and further increases in the field-aligned potential have no effect.

The acceleration of the magnetospheric electrons by the high-latitude field-aligned potential not only increases the field-aligned current density but also the energy of the precipitating electrons and the incident energy flux on the planetary atmosphere. This leads to enhancements in the ionospheric Pedersen conductance which, in turn, increase the angular momentum that is transferred from the planet to the magnetospheric plasma. The presence of field-aligned potentials also allows for differential rotation between the regions above and below the drop, i.e., the planetary magnetosphere and upper ionosphere, respectively.

3. NARROWNESS OF JUPITER'S MAIN AURORAL EMISSION

Understanding the interplay between the enhancement of the ionospheric Pedersen conductance and the development of field-aligned potentials is essential in describing the narrow

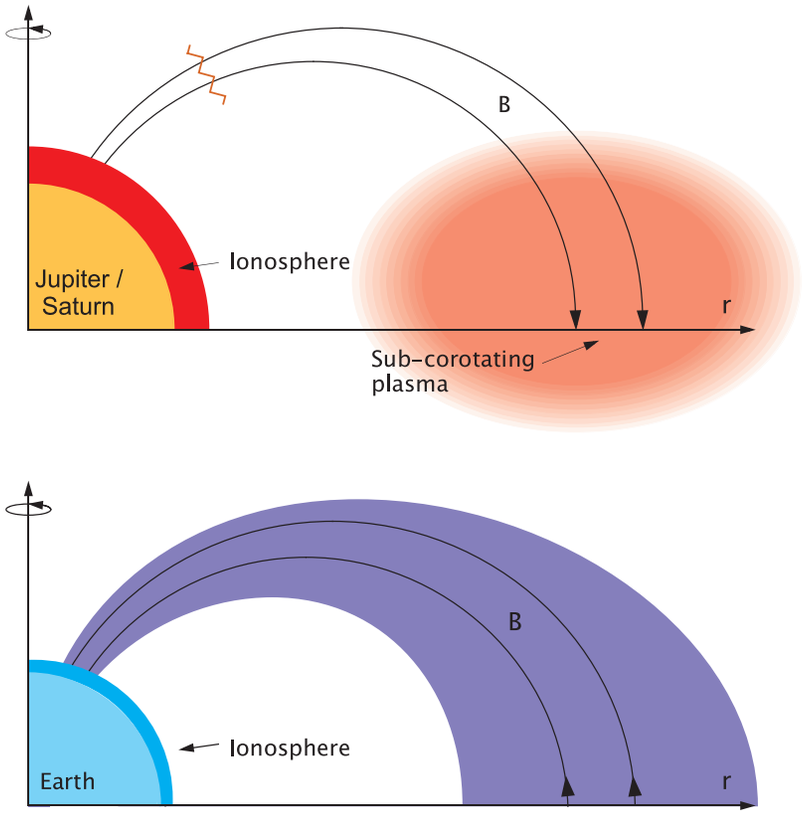

Figure 3. Cartoon of the plasma density distributions on Earth and Jupiter/Saturn. Jovian/Saturnian magnetospheric plasma is confined to the equatorial plane owing to the centrifugal confinement of the heavy ions and subsequent ambipolar electric field that develops.

main auroral emission observed on Jupiter. In the absence of field-aligned potentials, the ionosphere-magnetosphere system is perfectly coupled with the magnetosphere and upper ionosphere having the same rotation rate. However, once field-aligned potentials develop, the ionosphere and magnetosphere can differentially rotate, or slip, relative to each other. In a steady state system, the degree of differential rotation depends on the latitudinal derivative of the parallel potential, $\frac{d\Phi_{||}}{d\theta}$, following from $\nabla \times \mathbf{E} = 0$, i.e., how the field-aligned potential changes from one flux tube to the next when moving in planetary latitude or, equivalently, radial distance in the magnetosphere. When the latitudinal derivative of the field-aligned potential is positive, the magnitude of the ionospheric electric field increases relative to that of the magnetospheric electric field, and conversely, a negative latitudinal derivative is associated with a stronger magnetospheric electric field relative to the ionospheric field.

As the field-aligned potential and field-aligned current density increase, so does the electron precipitation into the planetary atmosphere, producing a bright aurora. The enhanced precipitation also increases the Pedersen conductance, which diminishes the magnitude of the ionospheric electric field. Meanwhile, the magnetospheric electric field decreases owing to the increased angular momentum transfer allowed by the enhanced Pedersen conductance and field-aligned current density. The final limitation on the magnetospheric plasma's demand for angular momentum is the planetary magnetic field. Jupiter's north-south equatorial magnetic field strength falls off faster than a dipole from ~15 to ~50 R_J as the inner portion of the ring current field acts to reduce the north-south component of the planetary magnetic field. The radial decrease in the magnetic field strength reduces the $\mathbf{J} \times \mathbf{B}$ force such that the magnetospheric plasma again begins to lag corotation. At the location where the magnitude of the magnetospheric electric field when mapped along the field lines to the planet exceeds that of the ionospheric electric field, the latitudinal derivative of the field-aligned potential changes sign. The field-aligned potential at high latitudes declines, and with it, the field-aligned current density and ionospheric Pedersen conductance also decrease. The electron precipitation energy and electron energy flux decrease limiting the poleward extent of the auroral emission, and a bright, narrow aurora of ~1°–2° is produced [*Ray et al.*, 2010, 2012].

4. SATURN'S DIFFUSE AURORAL EMISSION

Saturn's rotationally driven auroral emission may have two components: the diffuse emission that maps to a range of magnetospheric equatorial radii spanning 4–11 R_S, the bright ring of emission mapping to ~15 R_S, or a mixture of these two observed signatures. Saturn has a lower radial mass transport rate than Jupiter and a larger Pedersen conductance. Both of these factors should indicate a strong coupling between the ionosphere and magnetosphere. However, the magnetospheric angular velocities lag corotation outside ~3.3 R_S leading to the question: What limits the transfer of angular momentum from Saturn to its magnetospheric plasma?

One possibility is that Saturn's weaker magnetic field results in the Saturnian magnetosphere being more heavily mass loaded, relative to its magnetic energy content, than the Jovian magnetosphere [*Delamere et al.*, 2007; *Vasyliunas*, 2008] and perhaps prevents the ionosphere from ever being able to "grip" its magnetosphere. A second mechanism may be collisions between the magnetospheric ions and neutrals, which could contribute to the rotational lag of the magnetospheric plasma [*Saur et al.*, 2004]. Another limitation could be the lag in the rotation rate of the neutral atmosphere in the Pedersen conducting region at the planet as any neutral lag in corotation would be communicated to the magnetospheric plasma [*Huang and Hill*, 1989]. However, the neutral atmosphere would have to subcorotate by ~20% to be consistent with the observed magnetospheric flows, which would lead to strong, possibly unsustainable, atmospheric winds.

Last, inferred energy fluxes from the diffuse auroral emission would suggest that there are no strong field-aligned potentials, ($\Phi_{||} > \sim 3$ kV), at high latitudes inside of ~11 R_S [*Grodent et al.*, 2010]. There is a large abundance of protons in the Saturnian system relative to the Jovian system owing to water group-based chemistry. The magnetospheric protons have a smaller temperature anisotropy than the water group ions [*Wilson et al.*, 2008] and, therefore, more mobility along the magnetic field. As such, current flow between the ionosphere and magnetosphere may not be as restricted as in the Jovian system, adding to the mystery of Saturn's subcorotating magnetospheric plasma.

5. CONCLUSIONS

Planetary auroral emissions are excellent diagnostic tools of ionosphere-magnetosphere coupling. However, they often lead to more questions than they solve. By trying to reconcile in situ observations of the Jovian and Saturnian magnetospheres with auroral observations, we can develop and fine tune theoretical models of the ionosphere-magnetosphere interaction.

The strong internally driven auroral emission on Jupiter is a result of the interplay between the ionospheric Pedersen conductance and the lack of current-carrying plasma at high latitudes, results of both rapid rotation and an internal plasma population. Yet at Saturn, whether the broad, diffuse

emission and/or the higher latitude narrow, bright emission is the signature of the coupling between the magnetospheric plasma and planetary atmosphere remains an open question. Continued missions to the outer planets and auroral observing campaigns are the key to unlocking this mystery.

REFERENCES

Achilleos, N., C. S. Arridge, C. Bertucci, C. M. Jackman, M. K. Dougherty, K. K. Khurana, and C. T. Russell (2008), Large-scale dynamics of Saturn's magnetopause: Observations by Cassini, *J. Geophys. Res.*, *113*, A11209, doi:10.1029/2008JA013265.

Bagenal, F., and P. A. Delamere (2011), Flow of mass and energy in the magnetospheres of Jupiter and Saturn, *J. Geophys. Res.*, *116*, A05209, doi:10.1029/2010JA016294.

Bonfond, B. (2012), When moons create aurora: The satellite footprints on giant planets, in *Auroral Phenomenology and Magnetospheric Processes: Earth and Other Planets*, *Geophys. Monogr. Ser.*, doi:10.1029/2011GM001169, this volume.

Bonfond, B., D. Grodent, J.-C. Gérard, A. Radioti, V. Dols, P. A. Delamere, and J. T. Clarke (2009), The Io UV footprint: Location, inter-spot distances and tail vertical extent, *J. Geophys. Res.*, *114*, A07224, doi:10.1029/2009JA014312.

Bunce, E. J. (2012), Origins of Saturn's auroral emissions and their relationship to magnetosphere dynamics, in *Auroral Phenomenology and Magnetospheric Processes: Earth and Other Planets*, *Geophys. Monogr. Ser.*, doi:10.1029/2011GM001191, this volume.

Clarke, J. T. (2012), Auroral processes on Jupiter and Saturn, in *Auroral Phenomenology and Magnetospheric Processes: Earth and Other Planets*, *Geophys. Monogr. Ser.*, doi:10.1029/2011GM001199, this volume.

Clarke, J. T., D. Grodent, S. W. H. Cowley, E. J. Bunce, P. Zarka, J. E. P. Connerney, and T. Satoh (2004), Jupiter's aurora, in *Jupiter: The Planet, Satellites and Magnetosphere*, edited by F. Bagenal, T. E. Dowling, and W. B. McKinnon, pp. 639–670, Cambridge Univ. Press, Cambridge, U. K.

Cowley, S. W. H., and E. J. Bunce (2001), Origin of the main auroral oval in Jupiter's coupled magnetosphere-ionosphere system, *Planet. Space Sci.*, *49*, 1067–1088.

Cowley, S. W. H., and E. J. Bunce (2003), Corotation-driven magnetosphere-ionosphere coupling currents in Saturn's magnetosphere and their relation to the auroras, *Ann. Geophys.*, *21*, 1691–1707, doi:10.5194/angeo-21-1691-2003.

Cowley, S. W. H., J. D. Nichols, and D. J. Andrews (2007), Modulation of Jupiter's plasma flow, polar currents, and auroral precipitation by solar wind-induced compressions and expansions of the magnetosphere: a simple theoretical model, *Ann. Geophys.*, *25*, 1433–1463, doi:10.5194/angeo-25-1433-2007.

Cowley, S. W. H., C. S. Arridge, E. J. Bunce, J. T. Clarke, A. J. Coates, M. K. Dougherty, J.-C. Gérard, D. Grodent, J. D. Nichols, and D. L. Talboys (2008), Auroral current systems in Saturn's magnetosphere: Comparison of theoretical models with Cassini and HST observations, *Ann. Geophys.*, *26*, 2613–2630, doi:10.5194/angeo-26-2613-2008.

Delamere, P. A. (2012), Auroral signatures of solar wind interaction at Jupiter, in *Auroral Phenomenology and Magnetospheric Processes: Earth and Other Planets*, *Geophys. Monogr. Ser.*, doi:10.1029/2011GM001180, this volume.

Delamere, P. A., F. Bagenal, and A. Steffl (2005), Radial variations in the Io plasma torus during the Cassini era, *J. Geophys. Res.*, *110*, A12223, doi:10.1029/2005JA011251.

Delamere, P. A., F. Bagenal, V. Dols, and L. C. Ray (2007), Saturn's neutral torus versus Jupiter's plasma torus, *Geophys. Res. Lett.*, *34*, L09105, doi:10.1029/2007GL029437.

Ergun, R. E., L. Ray, P. A. Delamere, F. Bagenal, V. Dols, and Y.-J. Su (2009), Generation of parallel electric fields in the Jupiter–Io torus wake region, *J. Geophys. Res.*, *114*, A05201, doi:10.1029/2008JA013968.

Fleshman, B. L., P. A. Delamere, and F. Bagenal (2010), A sensitivity study of the Enceladus torus, *J. Geophys. Res.*, *115*, E04007, doi:10.1029/2009JE003372.

Galand, M., L. Moore, I. Mueller-Wodarg, M. Mendillo, and S. Miller (2011), Response of Saturn's auroral ionosphere to electron precipitation: Electron density, electron temperature, and electrical conductivity, *J. Geophys. Res.*, *116*, A09306, doi:10.1029/2010JA016412.

Gérard, J.-C., J. Gustin, D. Grodent, P. Delamere, and J. T. Clarke (2002), Excitation of the FUV Io tail on Jupiter: Characterization of the electron precipitation, *J. Geophys. Res.*, *107*(A11), 1394, doi:10.1029/2002JA009410.

Grodent, D., J. T. Clarke, J. Kim, J. H. Waite Jr., and S. W. H. Cowley (2003a), Jupiter's main auroral oval observed with HST-STIS, *J. Geophys. Res.*, *108*(A11), 1389, doi:10.1029/2003JA009921.

Grodent, D., J. T. Clarke, J. H. Waite Jr., S. W. H. Cowley, J.-C. Gérard, and J. Kim (2003b), Jupiter's polar auroral emissions, *J. Geophys. Res.*, *108*(A10), 1366, doi:10.1029/2003JA010017.

Grodent, D., J.-C. Gérard, A. Radioti, B. Bonfond, and A. Saglam (2008), Jupiter's changing auroral location, *J. Geophys. Res.*, *113*, A01206, doi:10.1029/2007JA012601.

Grodent, D., A. Radioti, B. Bonfond, and J.-C. Gérard (2010), On the origin of Saturn's outer auroral emission, *J. Geophys. Res.*, *115*, A08219, doi:10.1029/2009JA014901.

Gustin, J., J.-C. Gérard, D. Grodent, S. W. H. Cowley, J. T. Clarke, and A. Grard (2004), Energy-flux relationship in the FUV Jovian aurora deduced from HST-STIS spectral observations, *J. Geophys. Res.*, *109*, A10205, doi:10.1029/2003JA010365.

Gustin, J., S. W. H. Cowley, J.-C. Gérard, G. R. Gladstone, D. Grodent, and J. T. Clarke (2006), Characteristics of Jovian morning bright FUV aurora from Hubble Space Telescope/Space Telescope Imaging Spectrograph imaging and spectral observations, *J. Geophys. Res.*, *111*, A09220, doi:10.1029/2006JA011730.

Gustin, J., J.-C. Gérard, W. Pryor, P. D. Feldman, D. Grodent, and G. Holsclaw (2009), Characteristics of Saturn's polar atmosphere and auroral electrons derived from HST/STIS, FUSE and

Cassini/UVIS spectra, *Icarus*, *200*, 176–187, doi:10.1016/j.icarus.2008.11.013.

Hansen, C. J., L. Esposito, A. I. F. Stewart, J. Colwell, A. Hendrix, W. Pryor, D. Shemansky, and R. West (2006), Enceladus' water vapor plume, *Science*, *311*, 1422–1425, doi:10.1126/science.1121254.

Hess, S. L. G., and P. A. Delamere (2012), Satellite-induced electron acceleration and related auroras, in *Auroral Phenomenology and Magnetospheric Processes: Earth and Other Planets*, *Geophys. Monogr. Ser.*, doi:10.1029/2011GM001175, this volume.

Hill, T. W. (1979), Inertial limit on corotation, *J. Geophys. Res.*, *84*(A11), 6554–6558.

Hill, T. W. (2001), The Jovian auroral oval, *J. Geophys. Res.*, *106*(A5), 8101–8107.

Hill, T. W., and F. C. Michel (1976), Heavy ions from the Galilean satellites and the centrifugal distortion of the Jovian magnetosphere, *J. Geophys. Res.*, *81*(25), 4561–4565.

Hill, T. W., and V. M. Vasyliunas (2002), Jovian auroral signature of Io's corotational wake, *J. Geophys. Res.*, *107*(A12), 1464, doi:10.1029/2002JA009514.

Huang, T. S., and T. W. Hill (1989), Corotation lag of the Jovian atmosphere, ionosphere, and magnetosphere, *J. Geophys. Res.*, *94*(A4), 3761–3765.

Joy, S. P., M. G. Kivelson, R. J. Walker, K. K. Khurana, C. T. Russell, and T. Ogino (2002), Probabilistic models of the Jovian magnetopause and bow shock locations, *J. Geophys. Res.*, *107*(A10), 1309, doi:10.1029/2001JA009146.

Khurana, K. K. (2001), Influence of solar wind on Jupiter's magnetosphere deduced from currents in the equatorial plane, *J. Geophys. Res.*, *106*(A11), 25,999–26,016.

Knight, S. (1973), Parallel electric fields, *Planet. Space Sci.*, *21*, 741–750.

Mauk, B. H., D. G. Mitchell, R. W. McEntire, C. P. Paranicas, E. C. Roelof, D. J. Williams, S. M. Krimigis, and A. Lagg (2004), Energetic ion characteristics and neutral gas interactions in Jupiter's magnetosphere, *J. Geophys. Res.*, *109*, A09S12, doi:10.1029/2003JA010270.

McNutt, R. L., Jr., J. W. Belcher, J. D. Sullivan, F. Bagenal, and H. S. Bridge (1979), Departure from rigid co-rotation of plasma in Jupiter's dayside magnetosphere, *Nature*, *280*, 803.

Millward, G., S. Miller, T. Stallard, A. D. Aylward, and N. Achilleos (2002), On the dynamics of the Jovian ionosphere and thermosphere III. The modelling of auroral conductivity, *Icarus*, *160*, 95–107, doi:10.1006/icar.2002.6951.

Moore, L., I. Mueller-Wodarg, M. Galand, A. Kliore, and M. Mendillo (2010), Latitudinal variations in Saturn's ionosphere: Cassini measurements and model comparisons, *J. Geophys. Res.*, *115*, A11317, doi:10.1029/2010JA015692.

Nichols, J. D. (2011), Magnetosphere-ionosphere coupling in Jupiter's middle magnetosphere: Computations including a self-consistent current sheet magnetic field model, *J. Geophys. Res.*, *116*, A10232, doi:10.1029/2011JA016922.

Nichols, J. D., and S. W. H. Cowley (2004), Magnetosphere-ionosphere coupling currents in Jupiter's middle magnetosphere: Effect of precipitation-induced enhancement of the ionospheric Pedersen conductivity, *Ann. Geophys.*, *22*, 1799–1827.

Nichols, J. D., E. J. Bunce, J. T. Clarke, S. W. H. Cowley, J.-C. Gérard, D. Grodent, and W. R. Pryor (2007), Response of Jupiter's UV auroras to interplanetary conditions as observed by the Hubble Space Telescope during the Cassini flyby campaign, *J. Geophys. Res.*, *112*, A02203, doi:10.1029/2006JA012005.

Pontius, D. H., Jr., and T. W. Hill (1982), Departure from corotation of the Io plasma torus: Local plasma production, *Geophys. Res. Lett.*, *9*(12), 1321–1324.

Pontius, D. H., Jr., and T. W. Hill (2009), Plasma mass loading from the extended neutral gas torus of Enceladus as inferred from the observed plasma corotation lag, *Geophys. Res. Lett.*, *36*, L23103, doi:10.1029/2009GL041030.

Pryor, W. R., et al. (2011), The auroral footprint of Enceladus on Saturn, *Nature*, *472*, 331–333, doi:10.1038/nature09928.

Radioti, A., J.-C. Gérard, D. Grodent, B. Bonfond, N. Krupp, and J. Woch (2008), Discontinuity in Jupiter's main auroral oval, *J. Geophys. Res.*, *113*, A01215, doi:10.1029/2007JA012610.

Ray, L. C., Y.-J. Su, R. E. Ergun, P. A. Delamere, and F. Bagenal (2009), Current-voltage relation of a centrifugally confined plasma, *J. Geophys. Res.*, *114*, A04214, doi:10.1029/2008JA013969.

Ray, L. C., R. E. Ergun, P. A. Delamere, and F. Bagenal (2010), Magnetosphere-ionosphere coupling at Jupiter: Effect of field-aligned potentials on angular momentum transport, *J. Geophys. Res.*, *115*, A09211, doi:10.1029/2010JA015423.

Ray, L. C., R. E. Ergun, P. A. Delamere, and F. Bagenal (2012), Magnetosphere-ionosphere coupling at Jupiter: A parameter space study, *J. Geophys. Res.*, *117*, A01205, doi:10.1029/2011JA016899.

Saur, J. (2004), A model of Io's local electric field for a combined Alfvénic and unipolar inductor far-field coupling, *J. Geophys. Res.*, *109*, A01210, doi:10.1029/2002JA009354.

Saur, J., B. H. Mauk, A. Kaßner, and F. M. Neubauer (2004), A model for the azimuthal plasma velocity in Saturn's magnetosphere, *J. Geophys. Res.*, *109*, A05217, doi:10.1029/2003JA010207.

Sergis, N., et al. (2010), Particle pressure, inertial force, and ring current density profiles in the magnetosphere of Saturn, based on Cassini measurements, *Geophys. Res. Lett.*, *37*, L02102, doi:10.1029/2009GL041920.

Sittler, E. C., Jr., M. F. Blanc, and J. D. Richardson (2006), Proposed model for Saturn's auroral response to the solar wind: Centrifugal instability model, *J. Geophys. Res.*, *111*, A06208, doi:10.1029/2005JA011191.

Thomas, N., F. Bagenal, T. W. Hill, and J. K. Wilson (2004), The Io neutral clouds and plasma torus, in *Jupiter: The Planet, Satellites and Magnetosphere*, edited by F. Bagenal, T. E. Dowling, and W. B. McKinnon, pp. 561–591, Cambridge Univ. Press, Cambridge, U. K.

Vasyliunas, V. M. (2008), Comparing Jupiter and Saturn: Dimensionless input rates from plasma sources within the magnetosphere, *Ann. Geophys.*, *26*(6), 1341–1343, doi:10.5194/angeo-26-1341-2008.

Wilson, R. J., R. L. Tokar, M. G. Henderson, T. W. Hill, M. F. Thomsen, and D. H. Pontius Jr. (2008), Cassini plasma spectrometer thermal ion measurements in Saturn's inner magnetosphere, *J. Geophys. Res.*, *113*, A12218, doi:10.1029/2008JA013486.

Wilson, R. J., R. L. Tokar, and M. G. Henderson (2009), Thermal ion flow in Saturn's inner magnetosphere measured by the Cassini plasma spectrometer: A signature of the Enceladus torus?, *Geophys. Res. Lett.*, *36*, L23104, doi:10.1029/2009GL040225.

Yates, J. N., N. Achilleos, and P. Guio (2012), Influence of upstream solar wind on thermospheric flows at Jupiter, *Planet. Space Sci.*, *61*, 15–31, doi:10.1016/j.pss.2011.08.007.

R. E. Ergun, Laboratory for Atmospheric and Space Physics, Discovery Drive, Boulder, CO 80309, USA.

L. C. Ray, Space and Atmospheres Group, Department of Physics, Imperial College London, Prince Consort Road, London SW7 2AZ, UK. (l.ray@imperial.ac.uk)